Supporting Information for "A quantitative comparison of high latitude electric field models during a large geomagnetic storm"

L. Orr[1], A. Grocott[1], M.-T. Walach[1], G. Chisham[2], M.P. Freeman[2], M.M. Lam[2], R.M. Shore[2]

[1]Space and Planetary Physics, Lancaster University

[2]British Antarctic Survey

Contents of this file

1. Description of the AENeAS version of the Heelis model code

2. Figures S1 to S7

1. AENeAS version of Heelis code

The TIE GCM version of Heelis (used within AENeAS (?, ?)) uses similar equations to those defined in (Hairston & Heelis, 1990). It is parameterised using B_y (nT) and cross polar cap potential, Φ_{cp} (kV). IMF B_y is set to be in the range $-11 \leq B_y \leq 7$ in the northern hemisphere and $-7 \leq B_y \leq 11$ in the southern hemisphere. TIE GCM uses an expression of Kp to represent the cross polar cap potential.

$$\Psi_{cp} = 15 + 15Kp + 0.8Kp^2. \tag{1}$$

1.1. Initial equations

The center (origin) of the polar cap circle is offset from the geomagnetic poles by $offc$ along the magnetic noon-midnight line and D_c in the dawn-dusk direction. N.B. equations given in degrees are converted to radians in the TIE GCM code. The plus and minus ($\pm$) refers to the northern and southern hemisphere, respectively.

$$O_{ffc} = 1.1^{\circ}, \qquad \text{Offset of convection towards 0 MLT relative to magnetic pole.} \tag{2}$$

$$D_c = -0.08^{\circ} \pm 0.15B_y^{\circ}, \qquad \text{Offset of convection in radians towards 18 MLT.} \tag{3}$$

The parameter, r, describes the decay of the potential equatorward of the convection reversal boundary, (Hairston & Heelis, 1990). It is set to the value of -2.6 in TIE GCM from average AMIE results.

$$r = -2.6, \text{ Exponential fall-off of convection from convection radius.} \tag{4}$$

The convection flow reversal circle, θ_0, is similar to equation 1 in Hairston and Heelis (1990) and that defined in Siscoe (1982).

$$\theta_0 = -3.8^\circ + 8.48^\circ \Psi_{pc}^{0.1875}, \qquad \text{Convection reversal boundary.} \tag{5}$$

The potential at the maximum, minimum and centre of the convection pattern (o_{ffc}, D_c) are defined as ψ_m, ψ_e and Ψ_0 respectively. These equations are of the same form as equations in Hairston and Heelis (1990) but have different values (?, ?).

$$\psi_m = 0.44\Psi_{pc} \times 1000 = \psi_3 = \psi_4 = \psi_7 = \psi_8, \text{ Maximum potential in morning cell,} \tag{6}$$

$$\psi_e = -0.56\Psi_{pc} \times 1000 = \psi_1 = \psi_2 = \psi_5 = \psi_6, \text{ Minimum potential in evening cell.} \tag{7}$$

$$\Psi_0 = (-0.168 \mp 0.027 B_y)\Psi_{pc} \times 1000, \qquad \text{Potential at the centre.} \tag{8}$$

The dayside and nightside convection entrance, or zero potential line, ϕ_d and ϕ_n, are first defined in MLT such that $\phi = 0$ is noon, before converting to degree and then to radians. The local magnetic time dependencies are described by six angles, similar to those described in Heelis, Lowell, and Spiro (1982). The maximum locations are the minimum of $\pi/2$ or half way between the dayside and nightside zero potential lines.

$$\phi_d = (9.39 \mp 0.21 B_y - 12)15^\circ, \qquad \text{Dayside convection entrance} \tag{9}$$

$$\phi_n = (23.50 \mp 0.15 B_y - 12)15^\circ, \qquad \text{Nightside convection entrance} \tag{10}$$

$$\phi_{dp}^{mx} = \frac{1}{2}\min(\pi, \phi_n - \phi_d), \tag{11}$$

$$\phi_{np}^{mx} = \frac{1}{2}\min(\pi, \phi_d - \phi_n + 2\pi), \tag{12}$$

$$\phi_{nm}^{mx} = \phi_{dp}^{mx}, \tag{13}$$

$$\phi_{dm}^{mx} = \phi_{np}^{mx}. \tag{14}$$

1.2. Magnetic latitude and longitude

If *nlt* is the number of latitude points, $1 \leq \mathbf{lt} \leq nlt$. The resulting magnetic latitude θ_m is not equally spaced.

$$r0 = 6.37122e8 + 9.0e6, \tag{15}$$

$$r1 = 1.06e7, \tag{16}$$

$$\theta_{\mathbf{N}} = (\mathbf{lt} - 1)\left(\frac{\pi}{nlt}\right) - \frac{\pi}{2}, \tag{17}$$

$$\mathbf{hamh0} = r1|\tan\theta_{\mathbf{N}}| + r0\frac{|\tan\theta_{\mathbf{N}}|^{(2+2\times1.668)}}{(1+|\tan\theta_{\mathbf{N}}|^2)^{1.668}}, \tag{18}$$

$$\theta_{\mathbf{m}} = \mathbf{ylatm} = \{\arctan\left(\frac{hamh0}{r0}\right)^{\frac{1}{2}}, \text{ if } \theta_N > 0, -\arctan\left(\frac{hamh0}{r0}\right)^{\frac{1}{2}}, \text{ if } \theta_N < 0. \tag{19}$$

Poles are equal to $\theta_{\mathbf{N}}([\mathbf{1}, \mathbf{nlt}])$.

nlon is the number of longitude points, **lon** is 1 to *nlon*. Sunlons defines the Sun's longitude in dipole coordinates from date.

$$\phi_{\mathbf{m}} = \mathbf{ylonm} = \frac{2\pi(lon-1)}{nlon} - \pi - sunlons. \tag{20}$$

1.2.1. Auroral Circle Coordinates

$$O_c = (O_{ffc}^2 + D_C^2)^{\frac{1}{2}}, \tag{21}$$

$$\phi_{off} = aslonc = \arcsin\frac{D_c}{O_c}, \tag{22}$$

$$\theta = \mathbf{colat} = \arccos(\cos O_c \sin|\theta_{\mathbf{m}}| - \sin O_c \cos\theta_{\mathbf{m}} \cos(\phi_{\mathbf{m}} + \phi_{off})), \tag{23}$$

$$\phi_{\mathbf{a}} = \mathbf{alon} = (\mathbf{A}, 2\pi) - \pi, \tag{24}$$

where $\mathbf{A} = \arctan 2(\mathbf{X}, \mathbf{Y}) - \phi_{off} + 3\pi$, $\mathbf{X} = \sin(\phi_{\mathbf{m}} + \phi_{off})\cos\theta_{\mathbf{m}}$, and $\mathbf{Y} = \sin|\theta_{\mathbf{m}}|\sin O_c + \cos O_c \cos\theta_{\mathbf{m}} \cos(\phi_{\mathbf{m}} + \phi_{off})$.

1.2.2. Boundaries for longitudinal function:

$$\phi_4 = \phi_d + 10^{-6} - \min\left(\frac{\pi}{2}, \phi_{dm}^{mx}\right), \tag{25}$$

$$\phi_5 = \phi_d - 10^{-6} + \min\left(\frac{\pi}{2}, \phi_{dp}^{mx}\right), \tag{26}$$

$$\phi_6 = \phi_n + 10^{-6} - \min\left(\frac{\pi}{2}, \phi_{nm}^{mx}\right), \tag{27}$$

$$\phi_7 = \phi_n - 10^{-6} + \min\left(\frac{\pi}{2}, \phi_{np}^{mx}\right), \tag{28}$$

$$\phi_1 = \phi_5 - 2\pi, \tag{29}$$

$$\phi_2 = \phi_6 - 2\pi, \tag{30}$$

$$\phi_3 = \phi_7 - 2\pi, \tag{31}$$

$$\phi_8 = \phi_4 + 2\pi. \tag{32}$$

1.2.3. Ring current rotation to potential

TIE GCM is set to have no ring current rotation hence:

$$\mathbf{wk_2} = (\phi_{\mathbf{a}} + 5\pi, 2\pi) - \pi, \tag{33}$$

$$\mathbf{wk_3} = (\phi_{\mathbf{a}} + 6\pi, 2\pi) - \pi. \tag{34}$$

1.3. Longitudinal variation:

$$\mathbf{\Psi_{fun}} = \mathbf{\Psi_{fn2}} = 0 \tag{35}$$

For $n = 1$ to 7

$$\mathbf{\Psi_{fun}} = \mathbf{\Psi_{fun}} + \frac{1}{4}\left(\psi_n + \psi_{n+1} + (\psi_n - \psi_{n+1})\cos\left(\frac{\pi(\mathbf{wk_2} - \phi_n)}{\phi_{n+1} - \phi_n}\right)\right), \tag{36}$$

if $(\mathbf{wk_2} - \phi_n)(\mathbf{wk_2} - \phi_{n+1}) < 0$, or $\mathbf{\Psi_{fun}} = \mathbf{\Psi_{fun}}$ if $(\mathbf{wk_2} - \phi_n)(\mathbf{wk_2} - \phi_{n+1}) > 0$.

And

$$\mathbf{\Psi_{fn2}} = \mathbf{\Psi_{fn2}} + \frac{1}{4}\left(\psi_n + \psi_{n+1} + (\psi_n - \psi_{n+1})\cos\left(\frac{\pi(\mathbf{wk_3} - \phi_n)}{\phi_{n+1} - \phi_n}\right)\right), \tag{37}$$

if $(\mathbf{wk_3} - \phi_n)(\mathbf{wk_3} - \phi_{n+1}) < 0$ or $\mathbf{\Psi_{fn2}} = \mathbf{\Psi_{fn2}}$ if $(\mathbf{wk_3} - \phi_n)(\mathbf{wk_3} - \phi_{n+1}) > 0$.

1.4. Evaluate total potential:

Equations for the total potential are given below. Equation 38 gives the potential inside the polar cap and is the same as equation 4 provided in (Hairston & Heelis, 1990). Equation 39 is quite different from the trigonometric or Gaussian functions suggested as frequent expressions of the latitudinal distribution outside of the cap by (Hairston & Heelis, 1990).

Inside the polar cap:

$$\mathbf{\Psi_{tot}} = A\left(\frac{\theta}{\theta_0}\right)^3 + B\left(\frac{\theta}{\theta_0}\right)^2 + C\left(\frac{\theta}{\theta_0}\right) + \Psi_0, \tag{38}$$

where $A = \left(2(\Psi_0 - \mathbf{\Psi_{fun}}) + \frac{3}{4}(\mathbf{\Psi_{fun}} - \mathbf{\Psi_{fn2}})\right)$, $B = 3\left(\frac{1}{2}(\mathbf{\Psi_{fun}} + \mathbf{\Psi_{fn2}}) - \Psi_0\right)$ and $C = \frac{3}{4}(\mathbf{\Psi_{fun}} - \mathbf{\Psi_{fn2}})$.

Outside the polar cap:

$$\mathbf{\Psi_{tot}} = \mathbf{\Psi_{fun}}\left(\frac{\max(\sin\theta, \sin\theta_0)}{\sin\theta_0}\right)^r \times \exp\left(7\left(1 - \frac{\max(\sin\theta, \sin(\theta_0 + 0.1972))}{\sin(\theta_0 + 0.1972)}\right)\right). \tag{39}$$

Average amie results show r1=-2.6 for 11.3 degrees (0.1972 rad) beyond θ_0.

Figures S1 to S7

References

Hairston, M., & Heelis, R. (1990). Model of the high-latitude ionospheric convection pattern during southward interplanetary magnetic field using de 2 data. *Journal of Geophysical Research: Space Physics*, *95*(A3), 2333–2343.

Heelis, R., Lowell, J. K., & Spiro, R. W. (1982). A model of the high-latitude ionospheric convection pattern. *Journal of Geophysical Research: Space Physics*, *87*(A8), 6339–6345.

Siscoe, G. L. (1982). Polar cap size and potential: A predicted relationship. *Geophysical Research Letters*, *9*(6), 672–675.

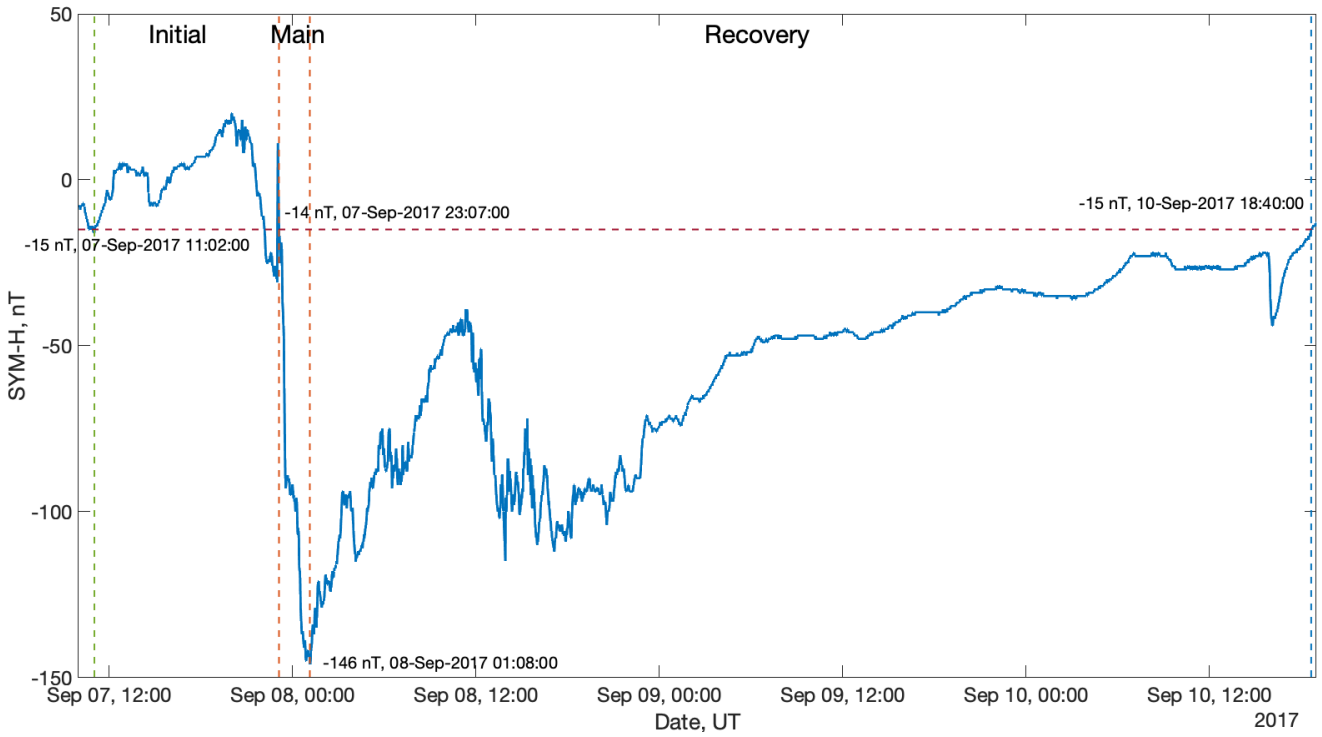

Figure S1. Sym-H for timings associated with TiVIE mode 3

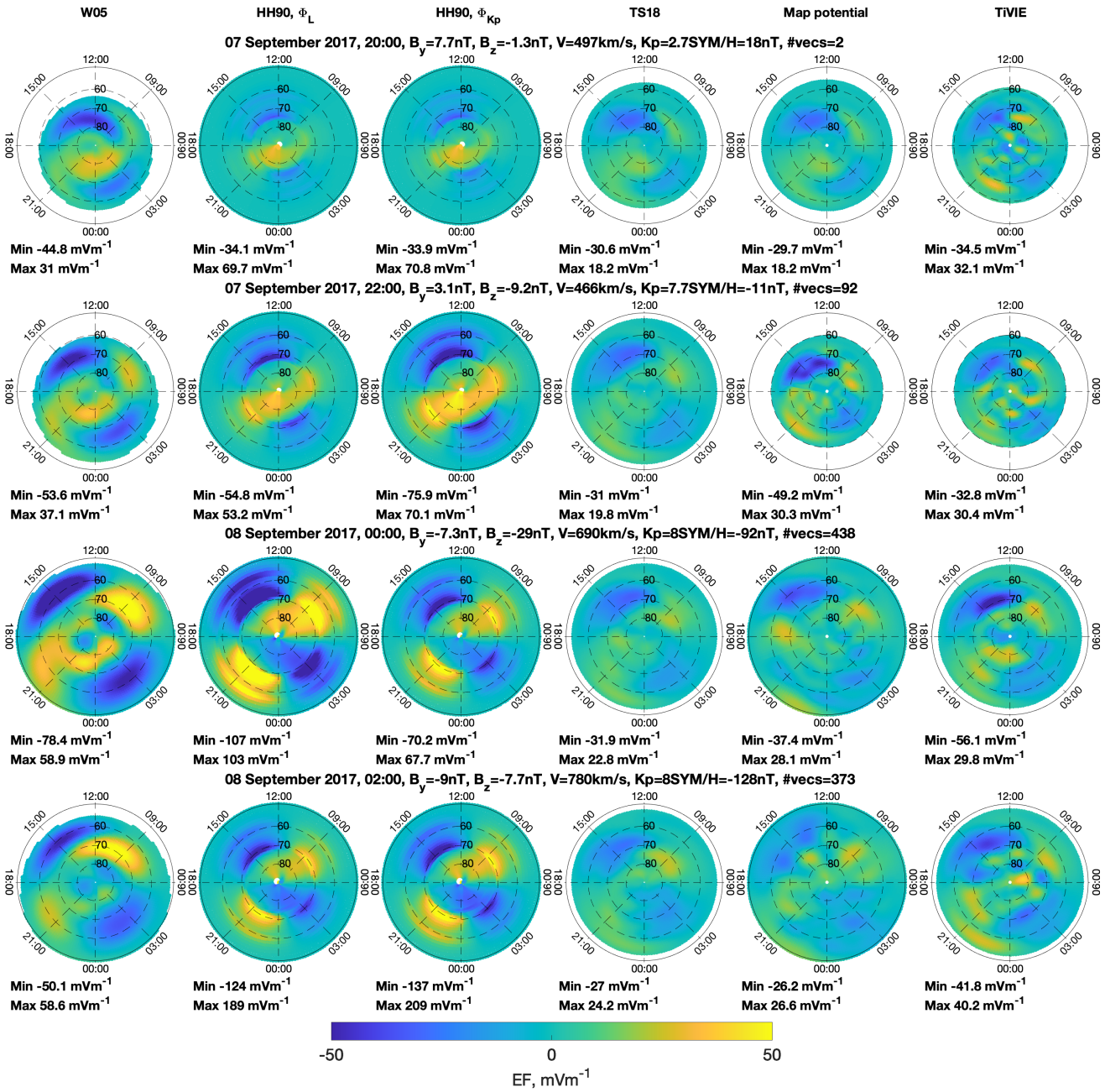

Figure S2. Midnight-to-noon directed component of the electric field vector in magnetic coordinates for the five models are four time intervals. Yellow represents positive, Midnight-to-noon directed electric field and blue negative, noon-to-midnight directed as shown in the colour bar. A selection of parameters including the time, IMF conditions, SW velocity, Kp, Sym/H and the number of SuperDARN vectors are provided per panel.

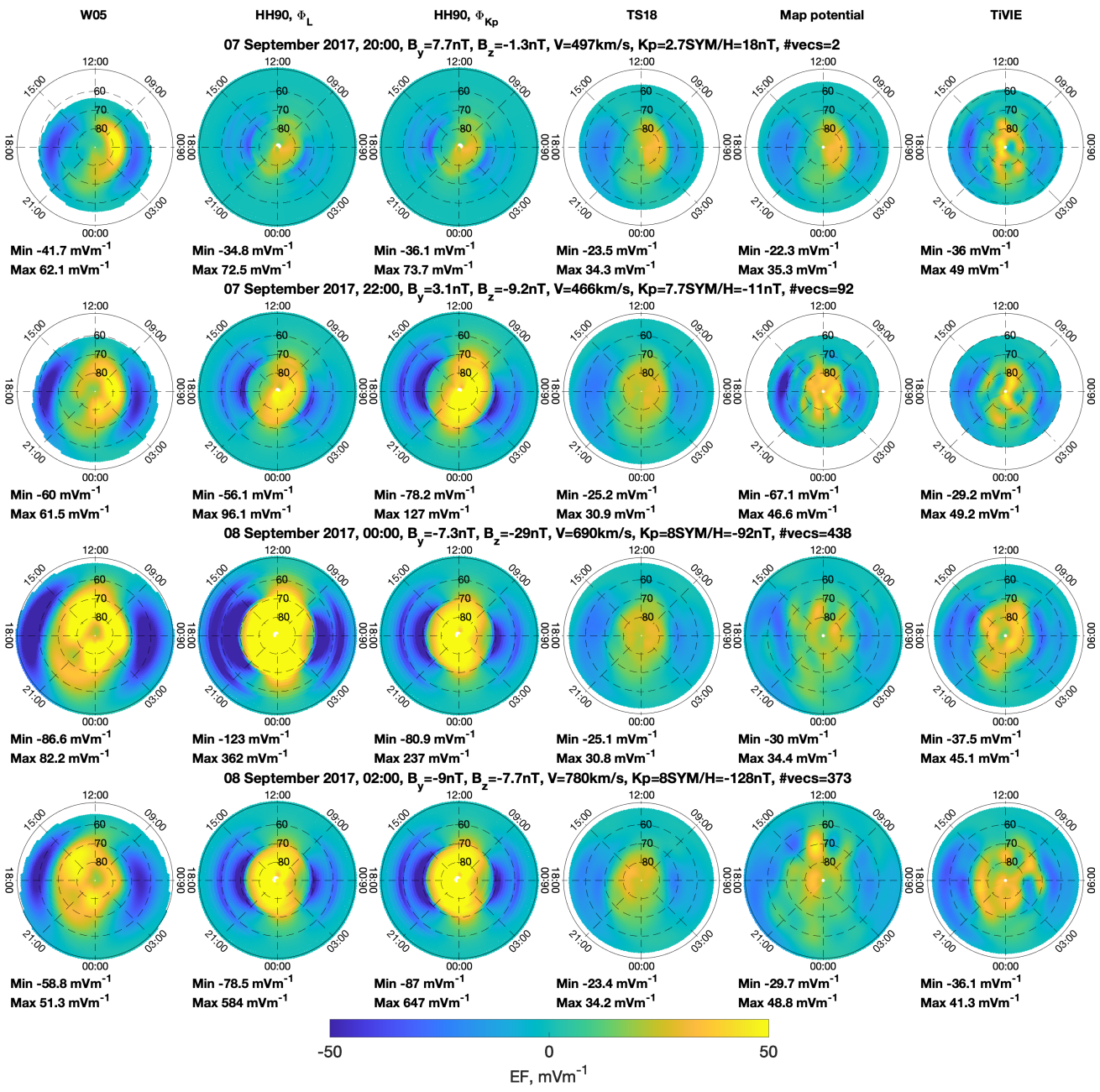

Figure S3. Dawn-to-dusk directed component of the electric field vector in magnetic coordinates for the five models are four time intervals. Yellow represents positive, Dawn-to-dusk electric field and blue negative, dusk-to-dawn directed as shown in the colour bar. A selection of parameters including the time, IMF conditions, SW velocity, Kp, Sym/H and the number of SuperDARN vectors are provided per panel.

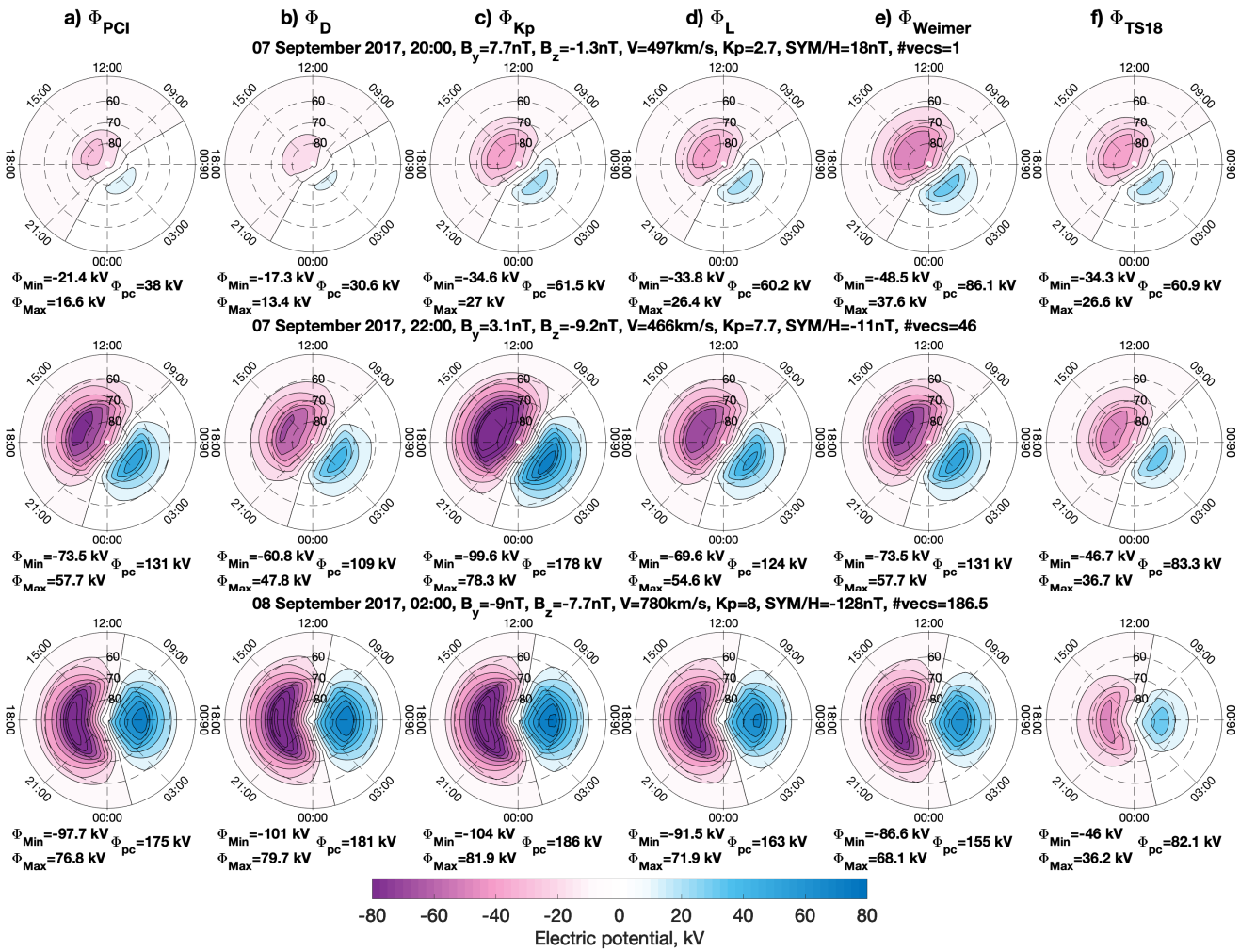

Figure S4. Convection maps in magnetic coordinates with contour lines representing 10kV intervals for the heelis model with six Φ_{PC} proxies are four time intervals. Purple/pink represents negative electric potential and blue positive, as shown in the colour bar. A selection of parameters including the time, IMF conditions, SW velocity, Kp, Sym/H and the number of SuperDARN vectors are provided per panel.

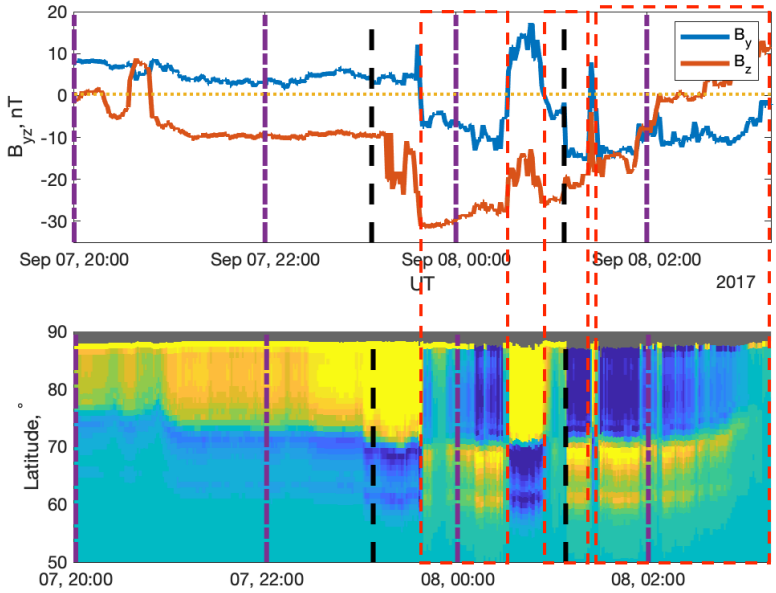

Figure S5. Figure highlighting the effect of the B_y component on the electric field north-south component from the Heelis model at midnight. A zoomed in version of figure 4, main text.

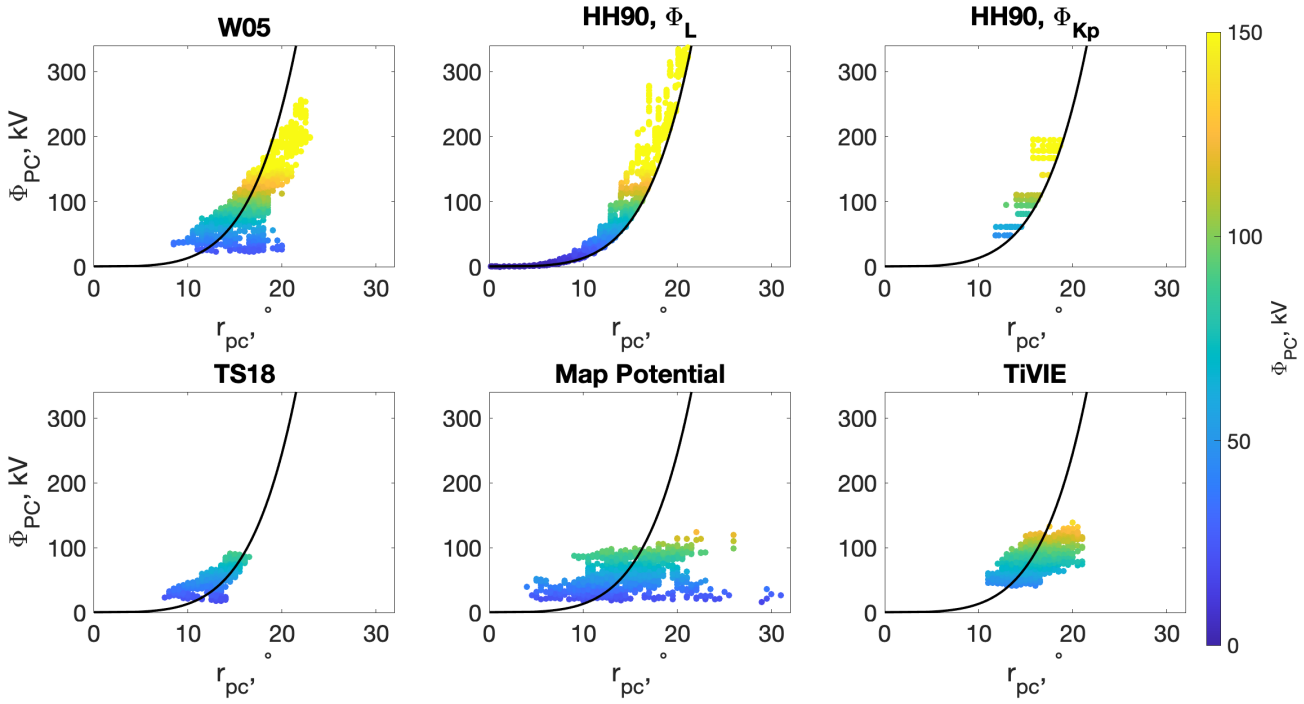

Figure S6. Proxy for the size of the polar cap, r_{pc} vs the cross polar cap potential, Φ_{PC}. The black line shows the trend the Heelis model uses for the convection reversal boundary.

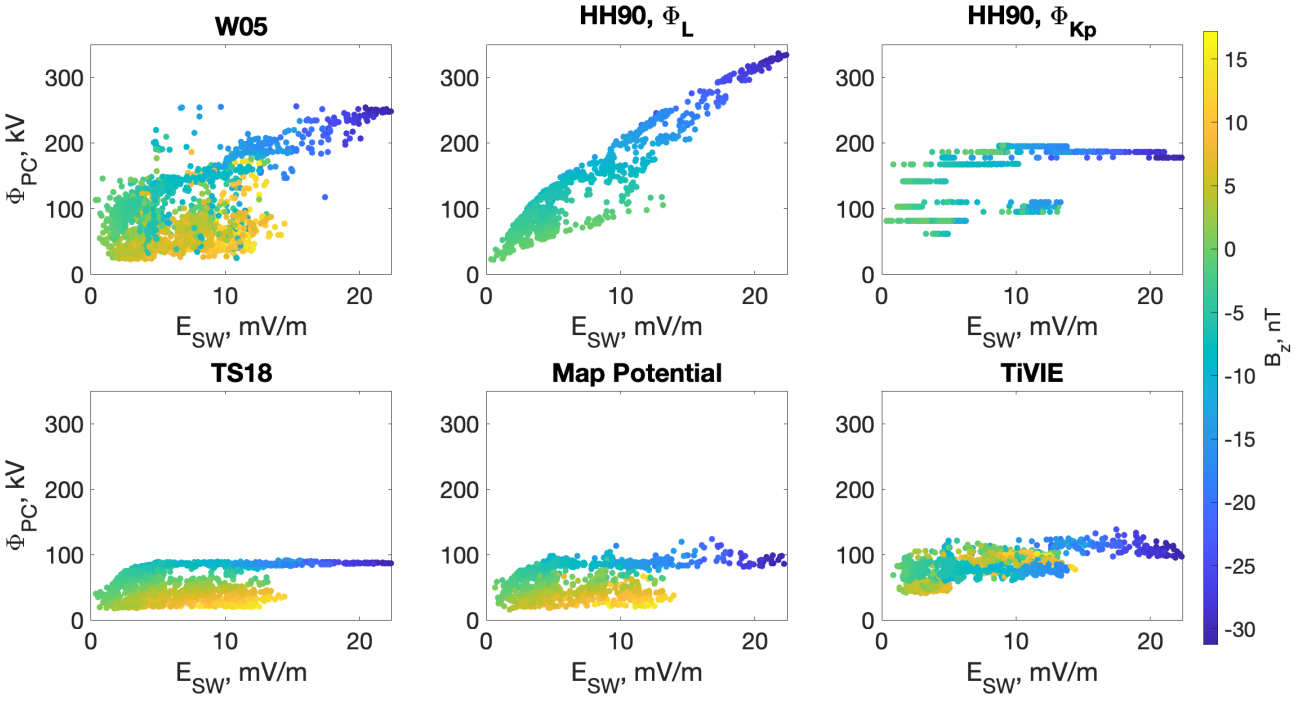

Figure S7. Scatter plot of E_{SW} vs Φ_{PC} with the colour representing B_z.